ELSEVIER

Ceramics International 32 (2006) 487–493

CERAMICS INTERNATIONAL

www.elsevier.com/locate/ceramint

Studies on the structural, electrical and optical properties of Al-doped ZnO thin films prepared by chemical spray deposition

Benny Joseph *, P.K. Manoj, V.K. Vaidyan

Department of Physics, University of Kerala, Trivandrum, Kerala 695 581, India

Received 1 January 2005; received in revised form 21 January 2005; accepted 27 March 2005
Available online 1 September 2005

Abstract

Aluminium-doped zinc oxide films have been prepared by chemical spray pyrolysis technique. Variation of structural, morphological, electrical and optical properties with doping concentration is investigated in detail. The films were highly transparent to visible radiation and electrically conductive. XRD studies have shown that the films were polycrystalline in nature with (0 0 2) preferred orientation. SEM studies have revealed the smooth polycrystalline morphology of the films. Films deposited at optimum conditions have exhibited a resistivity of 2.45×10^{-4} Ωm with an optical transmittance of 97% at 550 nm.

Keywords: Zinc oxide films; Aluminium doping; Spray pyrolysis; Transparent conducting films

1. Introduction

Zinc oxide (ZnO) is a multifunctional material with a wide area of applications. ZnO films have attracted considerable attention because they can be made to possess high electrical conductivity, high infrared reflectance and high visible transmittance. Low resistive zinc oxide films have been achieved by doping with different Group III elements like aluminium, boron, indium, gallium or with Group VII elements like fluorine [1–8]. Many techniques including evaporation, chemical vapour deposition, spray pyrolysis, sputtering, etc., can be employed to deposit these films [9–14]. For thin film applications like solar cell fabrication, spray pyrolysis technique is found attractive as it can deposit layers on large areas and provides itself easy to automation. The properties of the deposited material can be varied and controlled by proper optimization of spraying conditions.

In spray pyrolysis technique, low resistive ZnO films are obtained either by post-deposition heat treatment in vacuum or by hydrogen atmosphere or by adding donor impurities, such as aluminium or indium. In the present study, aluminium-doped zinc oxide (AZO) films have been prepared by using spray pyrolysis technique. The effects of aluminium doping on the structural, electrical and optical properties of AZO films have been reported.

2. Experimental

Aluminium-doped zinc oxide films were deposited on glass substrates by spray pyrolysis technique. The deposition method involves the decomposition of an aqueous solution of zinc acetate (0.1 M). The dopant concentration (Al/Zn at.%) was varied from 0 to 1.5 at.%. The resulting solution was sprayed onto the heated substrates at a constant temperature of 450 ± 5 °C. The temperature of the substrate was monitored by a chromel–alumel thermocouple close to the substrates. Compressed air was used as the carrier gas. To enhance the conductivity as-deposited films were annealed at 300 ± 5 °C

* Corresponding author at: Department of Physics, St. Joseph's College, Devagiri, Calicut, Kerala 673 008, India. Tel.: +91 495 2353772; fax: +91 495 2357370.
E-mail address: benny_chellamkottu@rediffmail.com (B. Joseph).

0272-8842/$30.00
doi:10.1016/j.ceramint.2005.03.029

for 90 min under a vacuum of 10^{-5} mbar. Films from acetate solution having molarity 0.2 and 0.4 M were also deposited at the optimum impurity concentration keeping the process parameters constant. The apparatus and deposition details have already been reported [15,16].

Characterization of the films was carried out using a Philips PW 1710 X-ray diffractometer (XRD) and a JOEL 35C scanning electron microscope (SEM). Film thickness was measured by the Tolansky's interferometric method. The resistivity studies were carried out using a four-probe set-up and the transmission studies using a Shimadzu double beam spectrophotometer UV240.

3. Results and discussion

3.1. Structural properties

Fig. 1 shows the X-ray diffraction patterns of AZO films with different aluminium concentrations deposited at substrate temperature 450 ± 5 °C. All the peaks in the pattern correspond to the hexagonal structure of ZnO powder sample and are indexed according to the ASTM data card 5-664. No phase corresponding to aluminium/aluminium oxide or other aluminium compound was detected in the XRD patterns. The preferential orientation of all films is found to be along (0 0 2) crystal plane. The other peaks observed in the X-ray diffractograms were (1 0 0), (1 0 1), (1 0 2), (1 0 3) and (1 1 2). Undoped ZnO films have exhibited (0 0 2) crystal plane preferential orientation [14]. An analysis has been carried out for the preferred orientation planes of the investigated thin films. The results have revealed the existence of the preferred (0 0 2) orientation with the *c*-axis perpendicular to the substrate surface. Such preferred basal orientation is typically observed in aluminium-doped ZnO films [17–19]. The lattice constants calculated from the most prominent peaks and the ratio of relative intensities $I(0\,0\,2)/I(1\,0\,1)$ in the diffraction pattern of AZO films at 450 ± 5 °C for different dopant concentrations are given in Table 1. The lattice constants calculated are found to be in good agreement with ASTM data for ZnO powder. The texture coefficient is calculated to describe the preferential orientation using the expression [20]:

$$\mathrm{TC}(h\,k\,l) = \frac{I(h\,k\,l)/I_0(h\,k\,l)}{N_r^{-1}\sum_{N_r} I(h\,k\,l)/I_0(h\,k\,l)} \quad (1)$$

where I is the measured intensity and I_0 is the measured standard intensity. The texture coefficient is calculated for the crystal planes (0 0 2) and (1 0 1). The value of the texture coefficient indicates the maximum preferred orientation of the films along the diffraction plane, meaning that the increase in preferred orientation is associated with increase in the number of grains along that plane. Fig. 2 represents the variation of TC(0 0 2) and TC(1 0 1) of ZnO films prepared at 450 ± 5 °C using 0.1 M zinc acetate solution for different aluminium concentrations.

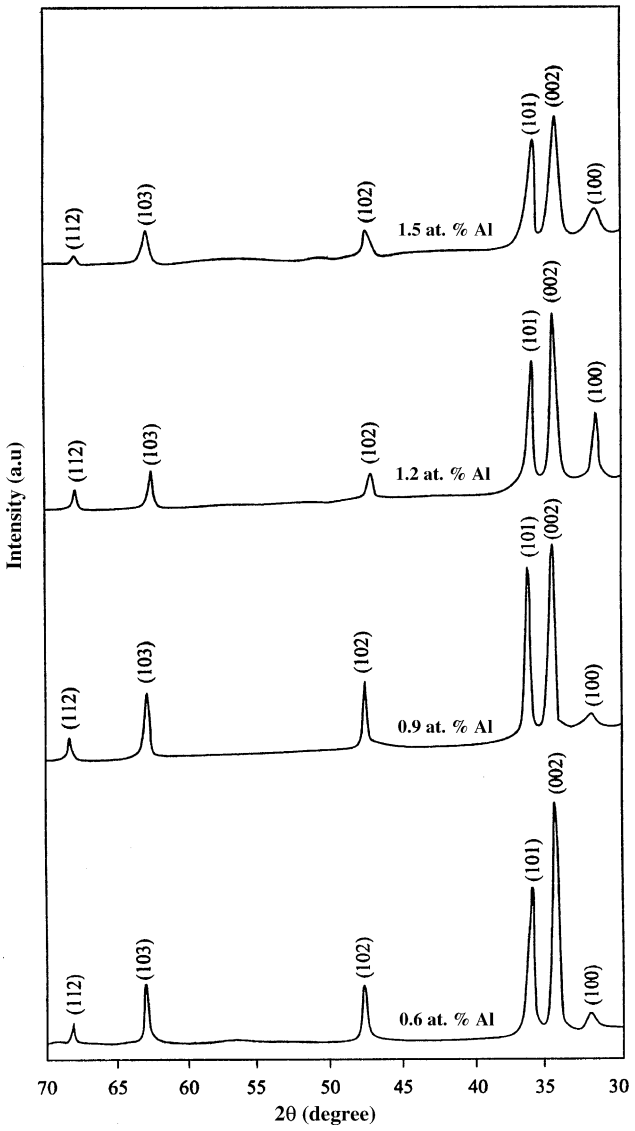

Fig. 1. XRD patterns of AZO films spray deposited at 450 ± 5 °C using 0.1 M zinc acetate solution with different aluminium concentrations.

Fig. 3 shows the X-ray diffractograms of AZO films deposited with different amounts of zinc acetate in the precursor solution. The preferential orientation of the AZO

Table 1
Lattice constants and $I(0\,0\,2)/I(1\,0\,1)$ ratios of zinc oxide films deposited at a substrate temperate 450±5 °C for different aluminium doping concentrations

Aluminium dopant concentration (at.%)	Lattice constants		Relative intensity $I(0\,0\,2)/I(1\,0\,1)$
	a_0 (nm)	c_0 (nm)	
0.6	0.3250	0.5198	1.628
0.9	0.3253	0.5202	1.098
1.2	0.3253	0.5208	1.311
1.5	0.3256	0.5200	1.167
ASTM	0.3249	0.5205	0.560

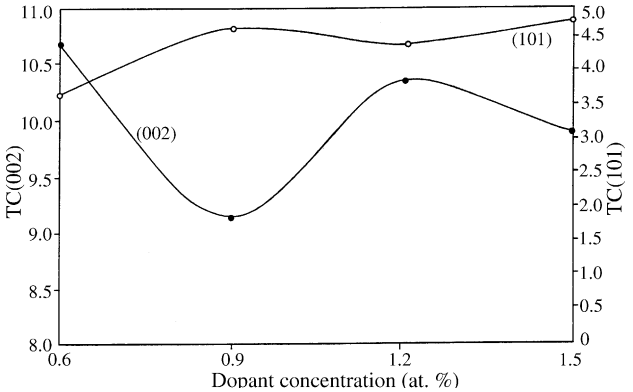

Fig. 2. Variation of texture coefficient TC(0 0 2) and TC(1 0 1) of zinc oxide films deposited at 450 ± 5 °C using 0.1 M zinc acetate solution with different aluminium, concentrations.

films is found to be along (0 0 2) and is found to improve with the molarity of the zinc acetate precursor solution. In spray pyrolysis decomposition, the impinging atoms on the substrate undergo endothermic reaction with substrate surface, resulting in a heterogeneous type of growth. Hence, one does not observe an oriented type of growth in the first few layers. As the thickness increases, this phenomenon becomes less and less effective and the arrangements of atoms in further layers gets gradually modified by the preceding layers. As a result, the growth takes place in a more definite way resulting in a particular type of preferred growth, along (0 0 2) direction. When the concentration of precursor solution increases, the film deposited includes the effects of increasing Zn incorporation, increasing growth rate as well as reorientational effects [21,22].

3.2. SEM studies

Fig. 4 shows the scanning electron micrograph of aluminium-doped zinc oxide films deposited at 450 ± 5 °C using 0.1 M zinc acetate solutions with different dopant concentrations. The micrographs show the uniform polycrystalline surface of the films. For small percentage of dopant concentration the micrograph shows no significant change in morphology.

3.3. Electrical and optical studies

The sheet resistance, resistivity, transmittance, optical band gap and figure of merit of zinc oxide films prepared under different deposition conditions, are given in Tables 2 and 3. The resistivity of as-deposited films lies in the range (1.6–2.6) × 10^{-2} Ωm. The aluminium doping has reduced the resistivity of undoped films by two orders of magnitude. To enhance the conductivity, as-deposited AZO films were annealed at 450 ± 5 °C for 90 min under a vacuum of 10^{-5} mbar. Vacuum annealing has resulted in the decrease of resistivity by two orders of magnitude. The low resistivity of

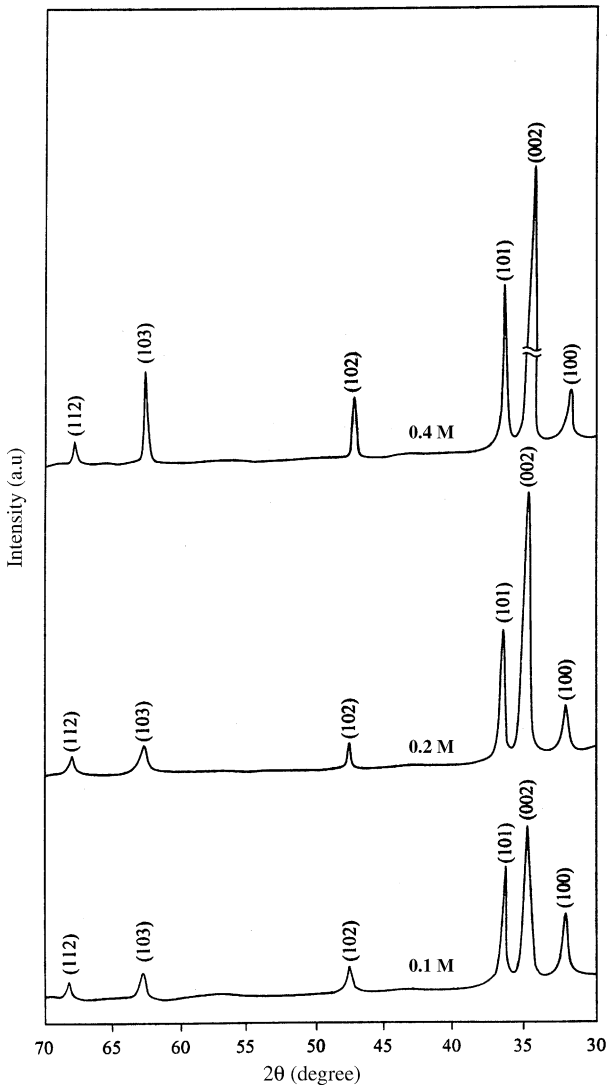

Fig. 3. XRD patterns of 1.2 at.% aluminium-doped zinc oxide films prepared at 450 ± 5 °C using zinc acetate solutions of different molarities.

AZO films is due to the combined effect of deviation from stoichiometry and aluminium doping. The resistivity of the film is found to decrease with aluminium concentration up to 1.5 at.%. The ionic radius of aluminium is smaller than that of zinc. The decrease in resistivity with the increase in dopant concentration is due to the replacement of Zn^{2+} by Al^{3+} ions. At higher doping concentrations, the disorder produced in the lattice increases the efficiency of scattering mechanism such as phonon scattering and ionized impurity scattering which in turn cause an increase in resistivity [23]. Small amounts of aluminium introduce large numbers of free electrons in the doped films, and the conductivity therefore increases. Further increase of aluminium concentration does not further increase the conductivity. This can be explained by the formation of nonconductive aluminium oxide from the extra aluminium atoms and the achievement of equilibrium between the aluminium atoms contributing conduction electrons and those producing aluminium oxide

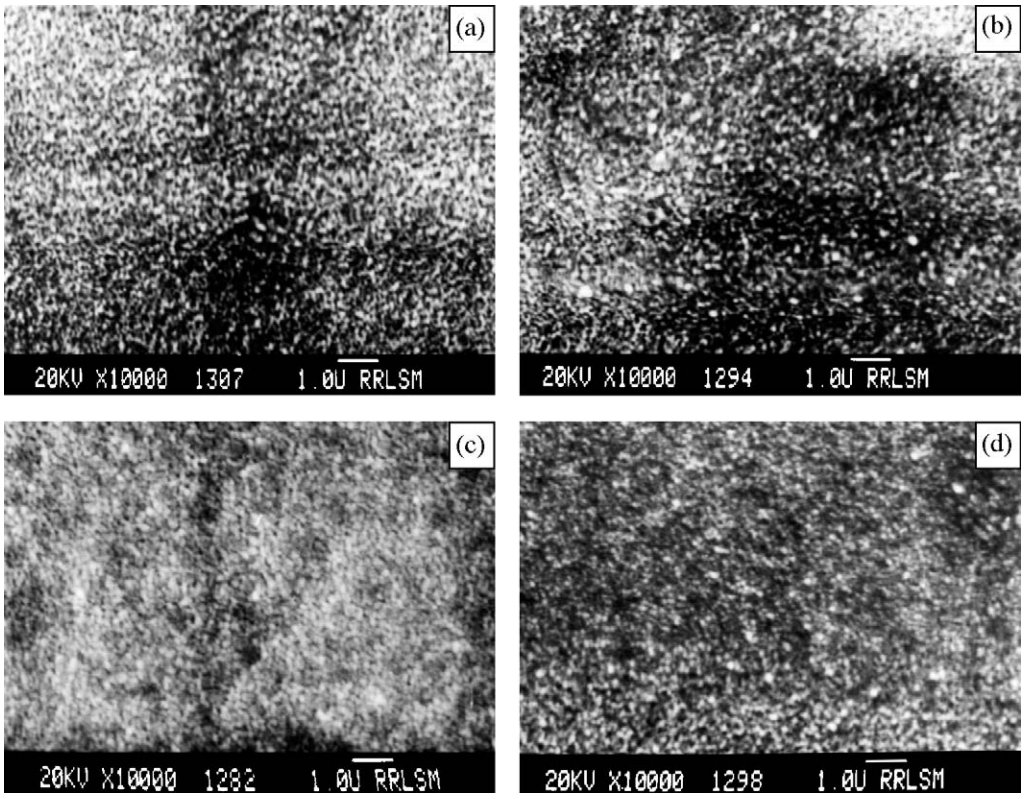

Fig. 4. SEM photographs of AZO films deposited at 450 ± 5 °C using 0.1 M zinc acetate solution with different aluminium concentrations: (a) 0; (b) 0.6; (c) 1.2; and (d) 1.5 at.%.

[18]. However, no aluminium phase was detected in the X-ray diffractograms. A minimum resistivity of 2.45×10^{-4} Ωm was obtained for films doped with 1.2 at.% aluminium. Films deposited at higher doping concentrations (>1.2 at.%) were of less transmittance, and the upper limit of doping concentration was fixed at 1.5 at.%.

Fig. 5 shows the optical transmission spectra of zinc oxide films prepared at substrate temperature of 450 ± 5 °C for different aluminium doping concentrations. The transmittance is found to decrease at 1.5 at.% of aluminium dopant concentration. The decrease of transmittance at higher doping levels (>1.2 at.%) may be attributed to the

Table 2
Electrical and optical properties of zinc oxide films prepared at 450 ± 5 °C using 0.1 M zinc acetate solutions with different aluminium dopant concentrations

Aluminium dopant concentration (at.%)	Sheet resistance before annealing ($\times 10^3$ Ω/□)	Resistivity before annealing (Ωm)	Sheet resistance after vacuum annealing ($\times 10^3$ Ω/□)	Resistivity after vacuum annealing (Ωm)	Transmittance at 550 nm (%)	Optical bandgap (eV)	Figure of merit (Ω^{-1})
0	9000	1.58	18	3.15×10	98	3.24	4.5×10
0.6	145	2.54×10^{-2}	14	2.45×10	93	3.27	3.5×10
0.9	130	2.28×10^{-2}	9	1.58×10	95	3.28	6.7×10
1.2	95	1.66×10^{-2}	1.4	2.45×10	97	3.28	5.3×10
1.6	100	1.75×10^{-2}	5.5	9.63×10	84	3.28	3.2×10

Table 3
Electrical and optical properties of AZO films deposited at 450 ± 5 °C using 1.2 at.% Al-doped zinc acetate solutions having different molarities

Molarity of solution (M)	Thickness (nm)	Sheet resistance before annealing ($\times 10^3$ Ω/□)	Resistivity before annealing (Ωm)	Sheet resistance after annealing ($\times 10^3$ Ω/□)	Resistivity after annealing (Ωm)	Transmittance at 550 nm (%)	Optical bandgap (eV)	Figure of merit (Ω^{-1})
0.1	175	95	1.66×10	1.40	2.45×10	97	3.28	5.3×10
0.2	300	78	2.34×10	1.23	3.69×10	86	3.28	1.8×10
0.4	450	70	3.15×10	1.10	4.95×10	84	3.28	1.6×10

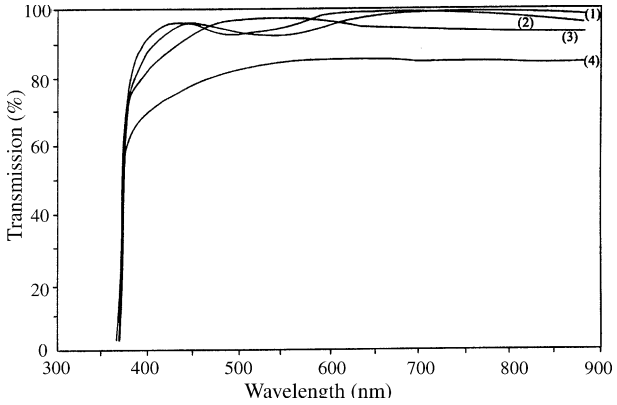

Fig. 5. Optical transmission spectra of aluminium-doped zinc oxide films deposited at a substrate temperature of 450 ± 5 °C using 0.1 M zinc acetate solution with different aluminium dopant concentrations: (1) 0.6 at.%; (2) 0.9 at.%; (3) 1.2 at.%; and (4) 1.6 at.%.

increased scattering of photons by crystal defects created by doping. The free carrier absorption of the photons may also contribute to the observed reduction in the optical transmission of heavily doped films [24]. The intrinsic absorption in a semiconductor occurs for wavelengths in the vicinity of the energy gap. The absorption coefficient α is calculated using Lambert's law.

$$\alpha = \frac{\ln(1/T)}{t} \tag{2}$$

where T is the transmittance and t, film thickness. The absorption is maximum at a high energy and decreases with optical energy in a manner similar to the absorption edge of semiconductors. Assuming that transition becomes constant at the absorption edge, the absorption coefficient α for directly allowed transition for simple parabolic scheme can be ascribed as a function of incident photon energy as [25]:

$$\alpha h\nu \propto (h\nu - E_g)^{1/2} \tag{3}$$

where E_g is the optical band gap. Fig. 6(a) and (b) show the typical $(\alpha h\nu)^2$ versus $h\nu$ graph of undoped zinc oxide films deposited at substrate temperature 450 ± 5 °C using 0.1 M zinc acetate solution with different dopant concentration (a) 0 at.% and (b) 1.2 at.%. The optical band gap has increased from 3.24 to 3.28 eV with aluminium dopant concentrations from 0 to 1.5 at.%. The change in optical band gap can be explained in terms of Burstein–Moss band gap widening and band gap narrowing due to the electron–electron and electron–impurity scattering [26–28].

Fig. 7 shows the transmission spectrum of 1.2 at.% aluminium-doped zinc oxide films deposited at 450 ± 5 °C, using zinc acetate precursor solutions of different molarities. The optical transmission spectra of the films show a decrease in transmittance with an increase in molarity of the precursor solution. The decrease in transmittance may be due to the increase in thickness of the films, resulting from the increase

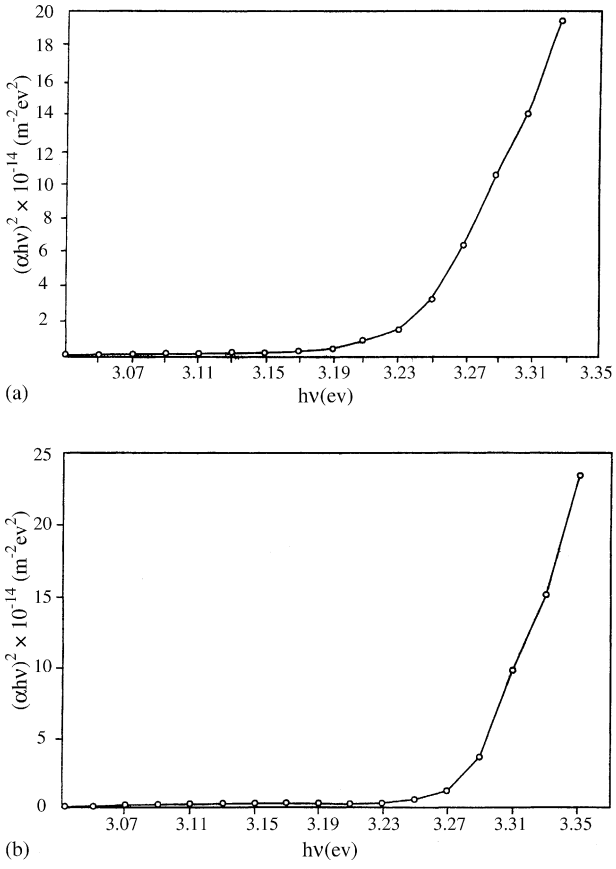

Fig. 6. Variation of $(\alpha h\nu)^2$ vs. $h\nu$ of ZnO films deposited at 450 ± 5 °C using 0.1 M zinc acetate solution with different aluminium dopant concentration: (a) 0 at.% and (b) 1.2 at.%.

of molarities of spraying solution. The variation of optical band gap of the film with thickness was not appreciable.

From the transmission spectrum alone, the refractive index $n(\lambda)$ of the films can be calculated using modified envelope method [29]. The envelope is drawn in the figure, and it is evident that for every wavelength λ there is a corresponding maximum transmittance T_M and minimum

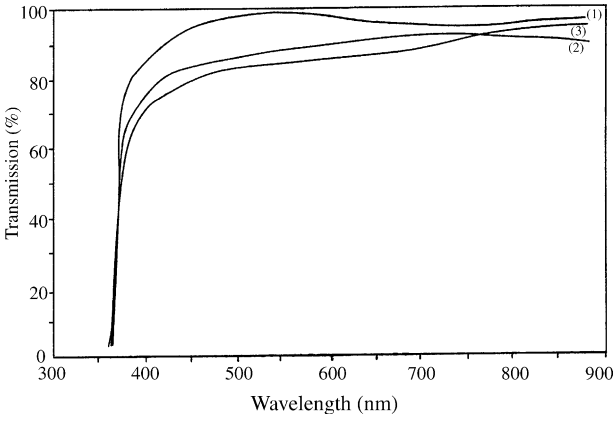

Fig. 7. Optical transmission spectra of 1.2 at.% aluminium-doped zinc acetate solutions of different molarities: (1) 0.1; (2) 0.2; and (3) 0.4 M.

transmittance T_m. The transmittance T is a function of the refractive index n, its extinction coefficient k and the thickness t of the film that has the general form

$$T = \frac{Ax}{B - Cx\cos\varphi + Dx^2} \tag{4}$$

where $A = 16n^2s$, $B = (n+1)^3(n+s^2)$, $C = 2(n^2-1)(n^2-s^2)$, $D = (n-1)^3(n-s^2)$, $\varphi = 4\pi nt/\lambda$.

$$k = \frac{\alpha\lambda}{4\pi} \tag{5}$$

where $x = \exp(-\alpha t)$ and s is the refractive index of the material of the substrate.

$$n = [N + (N^2 - s^2)^{1/2}]^{1/2} \tag{6}$$

where

$$N = \frac{1+s^2}{2} + \frac{8s^2}{(1+s)^2}\frac{T_M - T_m}{T_M T_m}$$

and

$$x = \frac{E_M - [E_M^2 - (n^2-1)^3(n^2-s^4)]^{1/2}}{(n-1)^3(n-s^2)} \tag{7}$$

where

$$E_M = \frac{8n^2s}{T_M} + (n^2-1)(n^2-s^2)$$

Once T_M and T_m are obtained from measured transmission spectrum, and the refractive index of the substrate is known, the refractive index of the film can be calculated from Eq. (6). Fig. 8 shows the plot of refractive index as a function of wavelength for different aluminium concentrations. The refractive index is found to decrease with the wavelength.

Most of the electronic applications require the films to have low absorption in the visible region and high dc conductivity. The figure of merit is defined as [30]:

$$\phi_{TC} = \frac{T^{10}}{R_\square} \tag{8}$$

where T is the transmittance and $R_\square$ is the sheet resistance. Tables 2 and 3 give the values of ϕ_{TC} of Al-doped zinc oxide films prepared under different deposition conditions. The highest value obtained for the figure of merit is $5.3 \times 10^{-4}\ \Omega^{-1}$ for films prepared under deposition conditions given in Table 4.

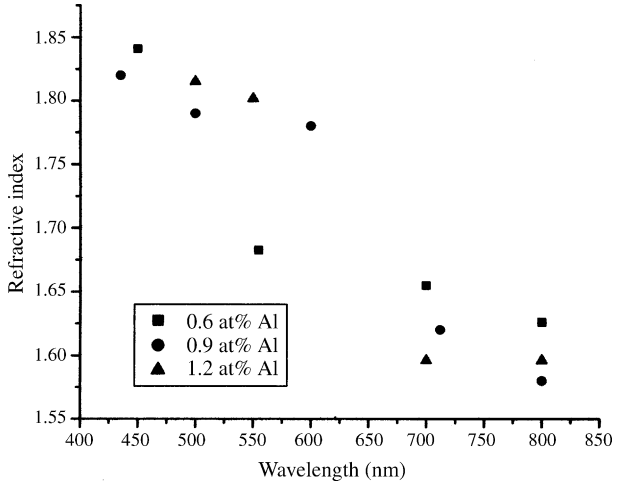

Fig. 8. Variation of refractive index with wavelength for films deposited at 450 ± 5 °C for different aluminium concentrations.

Table 4
Optimum spray conditions for the deposition of AZO films

Spray parameter	Optimum value/item
Zinc acetate solution concentration (M)	0.1
Solvent	Distilled water
Substrate temperature (°C)	450 ± 5
Carrier gas	Compressed air
Spray rate of the solution (ml/min)	5–6
Al/Zn dopant ratio (at.%)	1.2
Angular substrate to nozzle distance (cm)	44 ± 1

4. Conclusions

Aluminium-doped zinc oxide films have been successfully deposited by spray pyrolysis technique using a mixture of zinc acetate and aluminium chloride as precursor. The spray deposition of 1.2 at.% aluminium-doped 0.1 M zinc acetate solution at a substrate temperature of 450 ± 5 °C is found to be optimum for the deposition of good quality AZO films at the specified spray conditions. The films deposited at optimum conditions, exhibit an average transmittance of 94% in the visible region and a low resistivity of $2.45 \times 10^{-4}\ \Omega$m. The AZO films have shown a preferential orientation along (0 0 2) crystal plane and a smooth polycrystalline surface morphology irrespective of the deposition conditions.

References

[1] Y. Que, M.A. Gessert, K. Ramnathan, R.G. Dhere, R. Noufi, T.J. Coutts, J. Vac. Sci. Technol. A 11 (1993) 996.
[2] G.L. Harding, B. Window, E.E. Horrigan, Sol. Energy Mater. 22 (1991) 69.
[3] A. Sarkar, S. Gosh, S. Chaudhuri, A.K. Pal, Thin Solid Films 204 (1991) 255.
[4] K.H. Czternaste, A. Brudnik, M. Jachimowski, E. Kolawa, J. Phys. D: Appl. Phys. 25 (1992) 865.
[5] J. Hu, R.G. Gordon, J. Electrochem. Soc. 139 (1992) 2014.
[6] G.A. Hirata, J. Mckittrick, J. Siqueirors, O.A. Lopez, T. Cheeks, O. Contreras, J.Y. Yi, J. Vac. Sci. Technol. A 14 (1996) 791.
[7] D. Berhanu, D.S. Boyle, K. Govender, P. O'Brien, J. Mater. Sci.: Mater. Electon. 14 (2003) 579.
[8] T. Kawahara, T. Ishida, H. Tada, N. Toghe, S. Ito, J. Mater. Sci. Lett. 21 (2002) 1423.

[9] B. Joseph, K.G. Gopchandran, P.K. Manoj, J.T. Abraham, P. Koshy, V.K. Vaidyan, Indian J. Phys. 72A (1998) 99.
[10] N.D. Kumar, M.N. Kamalasanan, S. Chandra, Appl. Phys. Lett. 65 (1994) 1375.
[11] A. Tiburcio-Silver, J.C. Joubert, M. Labeau, Thin Solid Films 197 (1991) 195.
[12] S. Gosh, A. Sarkar, S. Chaudhuri, A.K. Pal, Vacuum 42 (1991) 195.
[13] S. Roy, S. Sabu, J. Mater. Sci.: Mater. Electron. 15 (2004) 321.
[14] R. Brenier, L. Ortega, J. Sol–gel Sci. Technol. 29 (2004) 137.
[15] B. Joseph, K.G. Gopachandran, P.V. Thomas, P. Koshy, V.K. Vaidyan, Mater. Chem. Phys. 58 (1999) 71.
[16] B. Joseph, K.G. Gopachandran, P.K. Manoj, P. Koshy, V.K. Vaidyan, Bull. Mater. Sci. 22 (1999) 921.
[17] A.F. Aktaruzzaman, G.L. Sharma, L.K. Malhotra, Thin Solid Films 198 (1991) 67.
[18] J. Hu, R.G. Gordon, J. Appl. Phys. 71 (1992) 880.
[19] T. Nakada, Y. Ohkubo, A. Kunioka, in: Proceedings of the IEEE 22nd Photovoltaic Specialists Conference, Las Vegas, USA, 1991, p. 548.
[20] C. Barret, T.B. Massalki, Structure of Metals, Pergamon, Oxford, 1980, p. 204.
[21] D.J. Goyal, C. Agasha, M.G. Takwale, B.R. Marathe, B.G. Bhide, J. Mater. Sci. Lett. 11 (1992) 708.
[22] C. Agasha, S.S. Major, Thin Film Characterization and Applications, Allied Publishers, New Delhi, 1996, p. 263.
[23] M. Mizuhashi, Thin Solid Films 76 (1980) 97.
[24] J.P. Upadhyay, S.R. Viswakarma, H.C. Prasad, Thin Solid Films 109 (1989) 195.
[25] A. Ables, Optical Properties of Solids, North Holland, Amsterdam, 1992, p. 32.
[26] E. Burstain, Phys. Rev. 93 (1954) 638.
[27] T.S. Moss, Proc. Phys. Soc. Lond.: Ser. B 67 (1954) 775.
[28] S.E. Sernelius, K.F. Berggren, Z.C. Jin, I. Hamberg, C.G. Granavist, Phys. Rev. B 37 (1988) 10244.
[29] C.H. Peng, S.B. Desu, J. Am. Ceramic. Soc. 77 (1994) 929.
[30] G. Haacke, J. Appl. Phys 247 (1976) 4086.